Department of Aerospace Engineering

Indian Institute of Technology, Bombay

Course project- **AE651**
Under guidance of Prof. A.M.Pradeep

Design of a Transonic Axial Fan

By

Deepak G D (183010033)

K Chacha Srihari(183010034)

TABLE OF CONTENTS

I. LIST OF TABLES

I. LIST OF FIGURES

1.Introduction

1.1 Axial compressors

Axial compressors are compressors in which the air flows mainly parallel to the rotational axis. Axial flow compressors have large mass flow capacity, high reliability, and high efficiencies, but have a smaller pressure rise per stage. A typical axial compressor has a series of rotating rotor blades followed by a stationary set of blades called stator that are concentric with the axis of rotation. The compressor blades/vanes are relatively flat in section. Each pair of rotors and stators is referred to as a stage as shown in fig-1. The stator blades are required in order to ensure reasonable efficiency. Without them, the gas would rotate with the rotor blades resulting in a large drop in efficiency. The axial compressor compresses the working fluid by first accelerating the air and then diffusing it to obtain a static pressure increase. The air is accelerated in the rotor and then diffused in the stator. The absolute velocity increases in the rotor and decreases in the diffuser. For successive stages, a saw-teeth pattern for the velocity is obtained, while the static pressure continuously increases in both of the rotor and stator rows of all stages.

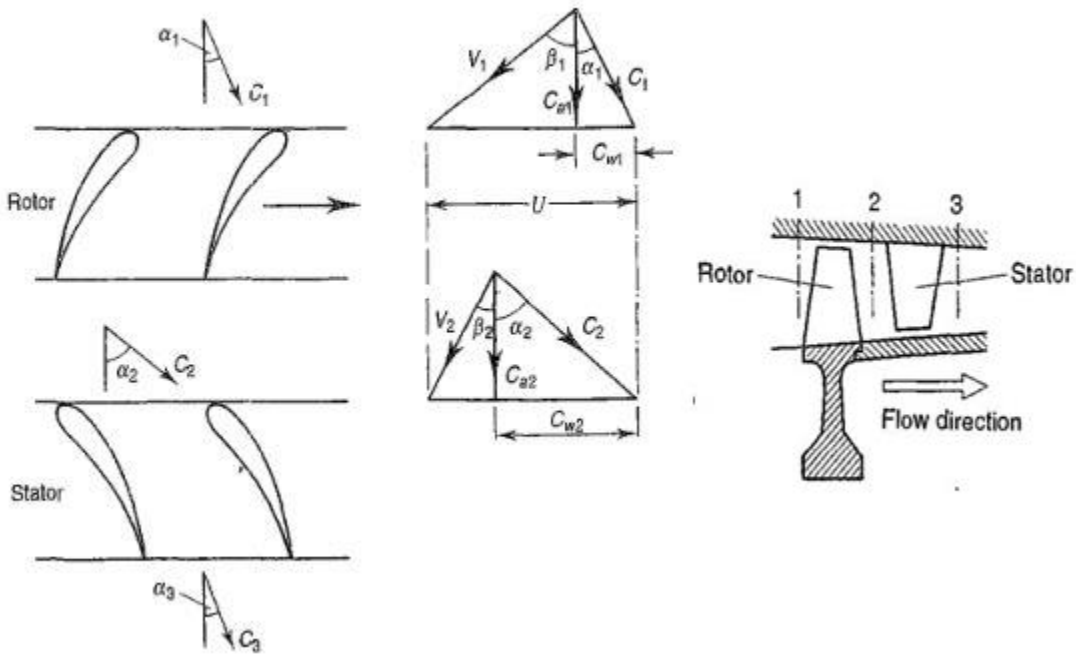

Figure 1-Layout of an axial compressor stage with velocity triangles[1]

Axial compressors are widely used in both aero-engines and industrial gas turbines. Almost all present-day jet engines use axial-flow compressors. The fan in turbofan engines is also an axial compression module which is treated as an axial compressor having a fewer number of blades of

very large height, wide chord, and large twist. Based on flow regime in the compressor, it may be classified as subsonic, transonic and supersonic compressors.

1.2 Transonic axial compressors

A transonic compressor is one where the relative flow remains subsonic at inner radii, supersonic at outer radii and transonic region in the middle. Transonic compressors are now successfully used in both aircraft and industrial gas turbines. The fan in turbofan engines is also an axial compression module which is more likely to be a transonic axial fan having a fewer number of blades of very large height, wide chord, and large twist. Early transonic and supersonic compressor designs were failures. The efficiencies were poor and the reliability was not good. It was initially believed that the low efficiencies obtained were due to the shock pattern alone. It was later recognized that the losses were more a result of flow disturbances caused by shocks. Major improvements have been made in blading design, shock optimization, and hub-to-tip design. The present airfoil blade designs are shown in fig-2. The most successful designs are the ones custom designed, based on the controlled diffusion airfoil and shock-free airfoil design concepts. This has enabled high efficiency to be achieved (from 40% in 1940's to nearly 90% currently) with various shock configurations (fig-2).

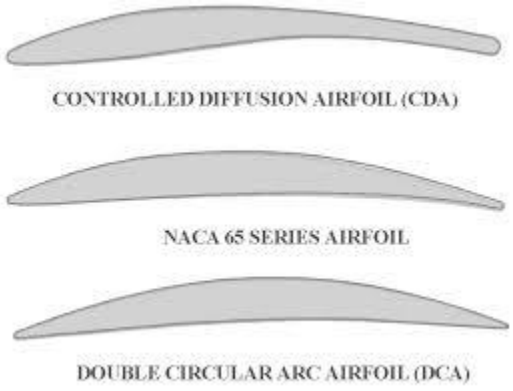

Figure 2-Transonic airfoils for axial compressor[3]

The present trend is towards low aspect ratio and higher Mach number blading, so as to achieve supersonic flow at most radial locations. The number of stages could be reduced for a given pressure ratio, thus enabling substantial savings in weight and size.

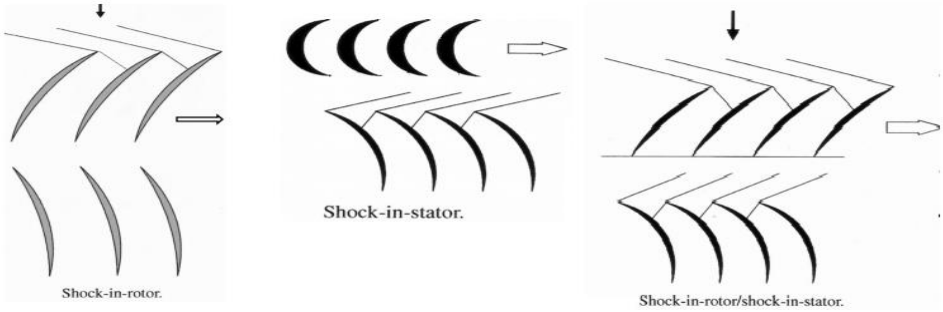

Figure 3-Various shock configurations in transonic compressors[5]

2.Design of Single-Stage Transonic Axial Fan

2.1 Problem statement

Design a single-stage transonic axial fan of following specifications.

Pressure ratio, π_c	1.5
Outer diameter (m)	0.8
Hub-tip ratio	0.4
Rotor speed, N (rpm)	10500
Mass flow rate (kg/s)	26

2.2 Design methodology:

2.2.1 Setting up the design criteria for transonic stage

- **$(\Delta T_0)_{transonic}$ = 45-55 K**

  The total temperature rise of the transonic stage is to be kept within this limit as per literature as mentioned in [4].If the rise is being either far beyond this range or much lower than this range, then the stage is more likely to become a supersonic or subsonic stage respectively.

- **$(M_{1rel})_{tip}$ = 1.1-1.7**

  The tip relative Mach number is to be kept within the above range. An increase above the upper threshold leads to unnecessary shock effects, leading to drastic efficiency drop.

- **$(D_h/D_t) \leq 0.4$**

  Since fans tend to handle larger mass flowrates, the hub to tip ratio is usually kept low and it is seen that the given specification itself is meeting this criteria by default.

- **$(\beta 1-\beta 2)$** is to be kept within reasonable limit (say $\leq 50°$)

  Since compressors operate under adverse pressure gradient, it is more likely to be prone to flow separation if flow turning is too large.

- **M_a = 0.4-0.7**

  The axial Mach number is to be kept in the above range. Alleviation from this design limit might lead to incidence losses.

2.2.2 Design step-by-step Procedure:

For designing the stage, Multall which is an open-source, CFD based, Turbomachinery design system is used with manually calculated properties (using spreadsheet) been given as input. Following flow-chart summarizes the design methodology in brief.

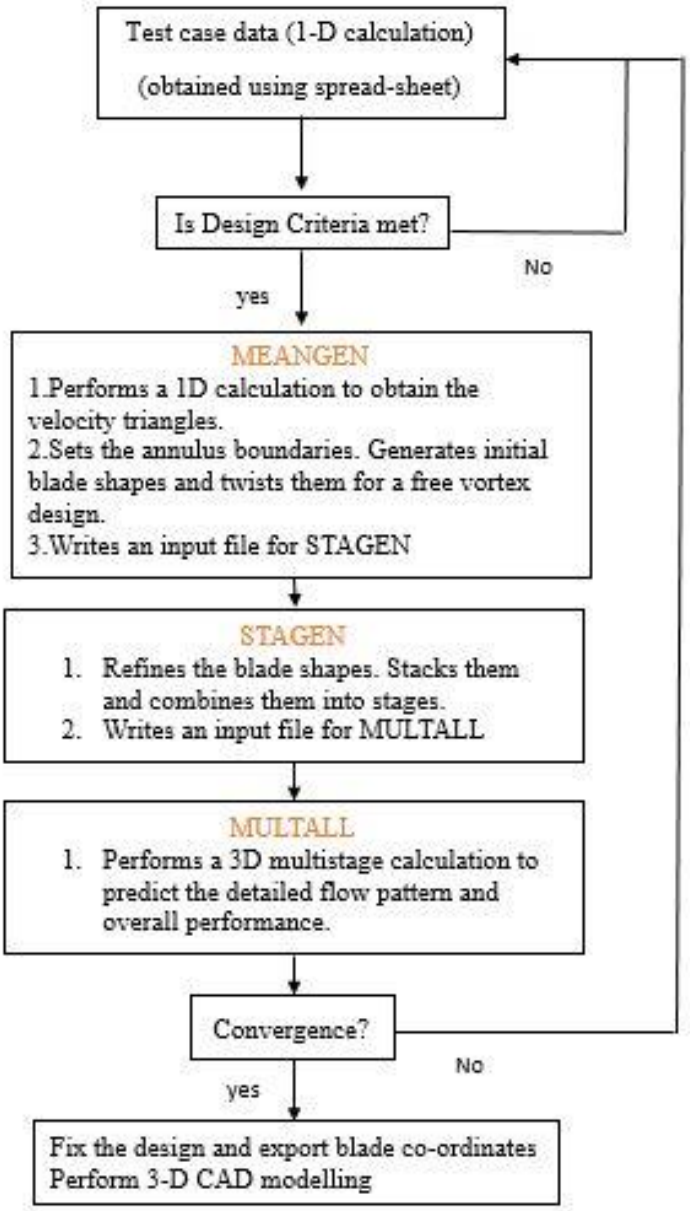

Figure 4-Flow chart describing the step-by-step design approach used

2.2.3 Mean-line Design

Given parameters

Pressure ratio, π_c	1.5
Outer diameter (m)	0.8
Hub-tip ratio	0.4
Rotor speed, N (rpm)	10500
Mass flow rate (kg/s)	26

Assumed parameters

Inlet static temperature,T_1(K)	294.6594
Inlet absolute Mach number,M_1	0.45
Compressor Efficiency, η_c(%)	90
α_1 (No IGV)	0°

Preliminarily, the design process involved calculation of various flow and blade parameters at the mean-section using empirical relations as follows.

The design is initiated by calculating the parameters at mean section as follows:

1. Inlet absolute velocity (C_1) is calculated from the assumed Mach number:

$$C_1 = M_1 * \sqrt{\gamma R T_1}$$

2. Axial absolute velocity is calculated from the inlet absolute velocity (C_1):

$$C_a = C_1 * \cos(\alpha_1)$$

3. Blade speed at mean diameter:

$$U_{mean} = \frac{\pi D_{mean} N}{60}$$

4. Work done on the fan/Compressor is calculated based on the pressure ratio & assumed efficiency:

$$\Delta h_0 = \frac{C_p T_{01}}{\eta_f}\left(\pi_c^{\frac{\gamma-1}{\gamma}} - 1\right)$$

5. Now, by equating Thermodynamic work and Aerodynamic work:

$$\Delta h_0 = U_{mean} C_a * \left(\tan(\alpha_2) - tan(\alpha_1)\right)$$

$$\alpha_2 = tan^{-1}\left(\frac{\Delta h_0}{U_{mean} C_a} + tan(\alpha_1)\right)$$

6. Using axial flow velocity and peripheral velocity, Flow coefficient is calculated:

$$\emptyset = \frac{C_a}{U_{mean}}$$

7. Blade angles at inlet and exit can be calculated by:

$$\frac{1}{\emptyset} = \frac{U_{mean}}{C_a} = \tan(\alpha_1) + tan(\beta_1) = \tan(\alpha_2) + tan(\beta_2)$$

$$\beta_1 = tan^{-1}\left(\frac{1}{\emptyset} - \tan(\alpha_1)\right)$$

$$\beta_2 = tan^{-1}\left(\frac{1}{\emptyset} - \tan(\alpha_2)\right)$$

8. Stage loading is calculated from stage enthalpy change and peripheral velocity:

$$\Psi = \frac{\Delta h_0}{{U_{mean}}^2}$$

9. Degree of Reaction is calculated from:

$$R_x = 1 - \frac{\emptyset}{2}\left(\tan(\alpha_2) + tan(\alpha_1)\right)$$

10. Diffusion Factor for Rotor & Stator:

$$D^*_{Rotor} = 1 - \frac{V_2}{V_1} + \frac{|V_{w1} - V_{w2}|}{2\left(\frac{C}{S}\right)V_1}$$

$$D^*_{Stator} = 1 - \frac{C_2}{C_1} + \frac{|C_{w1} - C_{w2}|}{2\left(\frac{C}{S}\right)C_1}$$

2.2.3.1 Mean-line Design: Test-cases: (1-5)

The above preliminary design calculations were made with 5 test cases which are shown in appendix -A. It was found that cases (1-4) cannot be carried out for further 3-D design approach, because of them being either not satisfying the transonic stage design criteria as discussed earlier or convergence criterion was not more likely to be met. But test-case (5), proved to be satisfying both the criteria and their respective aerodynamic parameters at the mean are carried out to the 3-D design. The design calculations for a sample test case (1) and for the finalized case (5), is shown below.

2.2.3.2 Mean line Design for Test Case-1

- Parameters given,
  - Single stage Transonic axial fan.
  - Pressure Ratio $\pi_f = 1.5$.
  - Outer Diameter D_0 = 0.8 m.
  - Hub-tip ratio = 0.4
  - Rotor Speed rpm = 10500
  - Mass flow $\dot{m} = 26$ kg/s.
- Assumptions made:
  - Inlet Static Temperature T_1 = 294.6594.
  - Inlet Absolute Mach number M_1 = 0.8.
  - Isentropic Efficiency of Fan $\eta_{st} = 0.9$
  - No inlet guide vanes (NGV) $\alpha_1 = 0^0$.
- From inlet absolute Mach number, M_1 = 0.8

$$C_1 = M_1\sqrt{\gamma R T_1}$$

$$C_1 = C_a = 275.26\ m/s$$

- Mean Peripheral Velocity (U_{mean}):

$$U_{mean} = \frac{\pi D_{mean} N}{60} = \frac{\pi * 0.56 * 10500}{60} = 307.8761\ m/s$$

- Work done / Stage enthalpy change from pressure ratio:

$$\Delta h_0 = \frac{C_p T_{01}}{\eta_f}\left(\pi_c{}^{\frac{\gamma-1}{\gamma}} - 1\right) = \frac{1005 * 332.357}{0.9}\left(1.5^{\frac{1.4-1}{1.4}} - 1\right) = 45.584\ KJ/kg$$

- Flow angle from stage enthalpy change:

$$\alpha_2 = tan^{-1}\left(\frac{\Delta h_0}{U_{mean} C_a} + tan(\alpha_1)\right) = tan^{-1}\left(\frac{45584.02}{307.8761 * 275.26} + tan(0)\right) = 28.27^0$$

- Flow Coefficient:

$$\emptyset = \frac{C_a}{U_{mean}} = \frac{275.26}{307.8761} = 0.89406$$

- Blade angles at inlet & exit of rotor:

$$\beta_1 = tan^{-1}\left(\frac{1}{\emptyset} - \tan(\alpha_1)\right) = tan^{-1}\left(\frac{1}{0.894} - \tan(0)\right) = 48.2^0$$

$$\beta_2 = tan^{-1}\left(\frac{1}{\emptyset} - \tan(\alpha_2)\right) = tan^{-1}\left(\frac{1}{0.894} - \tan(28.27)\right) = 30.13^0$$

- Stage Loading:

$$\Psi = \frac{\Delta h_0}{{U_{mean}}^2} = \frac{45584.02}{307.876^2} = 0.4809$$

- Degree of Reaction:

$$R_x = 1 - \frac{\emptyset}{2}\left(\tan(\alpha_2) + tan(\alpha_1)\right) = 1 - \frac{0.894}{2}\left(\tan(28.27) + tan(0)\right) = 0.7595$$

- Diffusion Factor for Rotor & Stator:

$$D^*_{Rotor} = 1 - \frac{V_2}{V_1} + \frac{|V_{w1} - V_{w2}|}{2\left(\frac{C}{S}\right)V_1} = 1 - \frac{318.29}{397.7} + \frac{|307.87 - 159.81|}{2 * \left(\frac{0.05}{0.025}\right) * 397} = 0.2927$$

$$D^*_{Stator} = 1 - \frac{C_2}{C_1} + \frac{|C_{w1} - C_{w2}|}{2\left(\frac{C}{S}\right)C_1} = 1 - \frac{312.56}{275.26} + \frac{|0 - 148.05|}{2 * \left(\frac{0.05}{0.025}\right) * 275.26} = 0.2732$$

2.2.3.3 Mean line Design for Test Case-5

- Parameters given,
  - Single stage Transonic axial fan.
  - Pressure Ratio $\pi_f = 1.5$.
  - Outer Diameter D_0 = 0.8 m.
  - Hub-tip ratio = 0.4
  - Rotor Speed rpm = 10500
  - Mass flow $\dot{m} = 26$ kg/s.
- Assumptions made:
  - Inlet Static Temperature T_1 = 294.6594.
  - Inlet Absolute Mach number M_1 = 0.45.
  - Isentropic Efficiency of Fan $\eta_{st} = 0.9$
  - No inlet guide vanes (NGV) $\alpha_1 = 0^0$.
- From inlet absolute Mach number, M_1 = 0.45

$$C_1 = M_1\sqrt{\gamma RT_1}$$

$$C_1 = C_a = 154.838\, m/s$$

- Mean Peripheral Velocity (U_{mean}):

$$U_{mean} = \frac{\pi D_{mean} N}{60} = \frac{\pi * 0.56 * 10500}{60} = 307.8761\, m/s$$

- Work done / Stage enthalpy change from pressure ratio:

$$\Delta h_0 = \frac{C_p T_{01}}{\eta_f}\left(\pi_c^{\frac{\gamma-1}{\gamma}} - 1\right) = \frac{1005 * 306.5872}{0.9}\left(1.5^{\frac{1.4-1}{1.4}} - 1\right) = 42.049\, KJ/kg$$

- Flow angle from stage enthalpy change:

$$\alpha_2 = tan^{-1}\left(\frac{\Delta h_0}{U_{mean} C_a} + tan(\alpha_1)\right) = tan^{-1}\left(\frac{42049.58}{307.8761 * 154.83} + tan(0)\right) = 41.41^0$$

- Flow Coefficient:

$$\emptyset = \frac{C_a}{U_{mean}} = \frac{154.838}{307.8761} = 0.503$$

- Blade angles at inlet & exit of rotor:

$$\beta_1 = tan^{-1}\left(\frac{1}{\emptyset} - \tan(\alpha_1)\right) = tan^{-1}\left(\frac{1}{0.503} - \tan(0)\right) = 63.3^0$$

$$\beta_2 = tan^{-1}\left(\frac{1}{\emptyset} - \tan(\alpha_2)\right) = tan^{-1}\left(\frac{1}{0.503} - \tan(41.41)\right) = 47.88^0$$

- Stage Loading:

$$\Psi = \frac{\Delta h_0}{{U_{mean}}^2} = \frac{42049.58}{307.876^2} = 0.4436$$

- Degree of Reaction:

$$R_x = 1 - \frac{\emptyset}{2}\left(\tan(\alpha_2) + tan(\alpha_1)\right) = 1 - \frac{0.503}{2}\left(\tan(41.41) + tan(0)\right) = 0.7781$$

- Diffusion Factor for Rotor & Stator:

$$D^*_{Rotor} = 1 - \frac{V_2}{V_1} + \frac{|V_{w1} - V_{w2}|}{2\left(\frac{C}{S}\right)V_1} = 1 - \frac{230.9}{322.4} + \frac{|307.87 - 171.29|}{2 * \left(\frac{0.05}{0.025}\right) * 322.4} = 0.4956$$

$$D^*_{Stator} = 1 - \frac{C_2}{C_1} + \frac{|C_{w1} - C_{w2}|}{2\left(\frac{C}{S}\right)C_1} = 1 - \frac{206.46}{154.83} + \frac{|0 - 136.57|}{2 * \left(\frac{0.05}{0.025}\right) * 154.83} = 0.423$$

3. 3-D Design: Using Free Vortex Law

Free vortex method is one of the simplest design methods in axial compressors. It is based on the general radial equilibrium equation with the following simplifications.

1. Assuming *constant specific work* at all radii, $\frac{dh_0}{dr} = 0$

$$\therefore C_a \frac{dC_a}{dr} + C_u \frac{dC_u}{dr} + \frac{C_u^2}{r} = 0$$

2. Assuming *constant axial velocity* at all radii, $\frac{dC_a}{dr} = 0$

$$\therefore C_u \frac{dC_u}{dr} + \frac{C_u^2}{r} = 0$$

$$\frac{dC_u}{C_u} = -\frac{dr}{r}$$

Figure 5- Free vortex law assumptions[4]

Integrating, we get

$$\boldsymbol{r.c_u = constant}$$

Thus the whirl velocity component of the flow varies inversely with radius, which is known as free vortex. Thus, the following three variables (h_0,C_a,r.C_u) are not varying in the radial direction. Keeping these implications, free vortex law is used to calculate flow properties along the annulus at the rotor inlet and outlet as shown below.

- The tangential absolute velocity along the annulus is calculated using,

$$\boldsymbol{r.c_u = r_m.c_m}$$

- The absolute flow angles at rotor inlet and outlet along annulus are calculated by,

$$\mathbf{r.\tan(\alpha_1)_r = r.\tan(\alpha_1)_m}$$

- The relative flow angles at rotor inlet and outlet along annulus are calculated from,

$$\mathbf{\tan(\alpha_1)_r + \tan(\beta_1)_r = \frac{Ur}{(Ca)r}},$$ where Ur = Um.$(\frac{D}{Dm})$

The results obtained in the spread-sheet are compared with the 'Stagen' results and by comparison, both are found to be matching each other. Various data were tabulated and plotted to check the feasibility of design and to have a clear-cut view of variation of various aerodynamic parameters as shown below.

Table 1- 3-D design using free vortex law

Variables						Sectional radius						
	Hub						Mean					Tip
r(m)	0.16	0.18	0.2	0.22	0.24	0.26	0.28	0.3	0.32	0.34	0.36	0.38	0.4
cu1(m/s)	0	0	0	0	0	0	0	0	0	0	0	0	0
cu2(m/s)	239.0142	212.4571	191.2114	173.8285	159.3428	147.0857	136.5795	127.4742	119.5071	112.4773	106.2285	100.6376	95.60568
R(r/rm)	0.571429	0.642857	0.714286	0.785714	0.857143	0.928571	1	1.071429	1.142857	1.214286	1.285714	1.357143	1.428571
U1(m/s)	175.9292	197.9203	219.9115	241.9026	263.8938	285.8849	307.8761	329.8672	351.8584	373.8495	395.8407	417.8318	439.823
U2(m/s)	175.9292	197.9203	219.9115	241.9026	263.8938	285.8849	307.8761	329.8672	351.8584	373.8495	395.8407	417.8318	439.823
Rx	0.320709	0.463276	0.565254	0.640706	0.698093	0.742754	0.778191	0.806779	0.830177	0.849569	0.865819	0.879572	0.891313
ca1(m/s)	154.838	154.838	154.838	154.838	154.838	154.838	154.838	154.838	154.838	154.838	154.838	154.838	154.838
ca2(m/s)	154.838	154.838	154.838	154.838	154.838	154.838	154.838	154.838	154.838	154.838	154.838	154.838	154.838
ΔT0(K)	41.84037	41.84037	41.84037	41.84037	41.84037	41.84037	41.84037	41.84037	41.84037	41.84037	41.84037	41.84037	41.84037
UΔcw(J/kg)	42049.57	42049.57	42049.57	42049.57	42049.57	42049.57	42049.57	42049.57	42049.57	42049.57	42049.57	42049.57	42049.57
α1(°)	0	0	0	0	0	0	0	0	0	0	0	0	0
α2(°)	57.06406	53.91556	51.00035	48.3069	45.82146	43.52917	41.41488	39.46377	37.66169	35.99537	34.45255	33.02201	31.69351
β1(°)	48.64849	51.96304	54.85092	57.37734	59.59799	61.5596	63.30112	64.85488	66.24773	67.50203	68.63643	69.66656	70.60558
β2(°)	-22.1673	-5.36341	10.50093	23.73257	34.02833	41.87356	47.88901	52.5827	56.32066	59.35732	61.86929	63.98074	65.78053
β1-β2(°)	70.81575	57.32645	44.34999	33.64478	25.56966	19.68604	15.41211	12.27218	9.927071	8.144708	6.767136	5.685818	4.825047
Vrel_1	225.5561	240.7002	256.4006	272.5209	288.9543	305.6163	322.4405	339.3741	356.3747	373.4087	390.4487	407.4726	424.4624
Vrel_2	167.1961	155.5189	157.4754	169.1416	186.8307	207.9424	230.9054	254.8288	279.2166	303.7931	328.4052	352.9688	377.4392
Vu_1	175.9292	197.9203	219.9115	241.9026	263.8938	285.8849	307.8761	329.8672	351.8584	373.8495	395.8407	417.8318	439.823
Vu_2	-63.085	-14.5367	28.70013	68.07412	104.551	138.7993	171.2965	202.393	232.3513	261.3723	289.6121	317.1943	344.2173
C_2	284.7852	262.8932	246.0418	232.7899	222.1822	213.5626	206.4674	200.5604	195.5933	191.3791	187.7746	184.6692	181.976
Solidity_R	1.601497	1.671127	1.281197	1.164725	1.067664	0.985536	0.915141	0.854132	0.800748	0.753645	0.711776	0.674314	0.640599
Solidity_S	3.342254	2.970892	2.673803	2.43073	2.228169	2.056772	1.909859	1.782535	1.671127	1.572825	1.485446	1.407265	1.336902
D*_R	0.589575	0.617982	0.67686	0.653166	0.611674	0.563766	0.515311	0.469003	0.425901	0.386273	0.350022	0.316895	0.286587
D*_S	0.581855	0.547034	0.516011	0.488459	0.464036	0.442405	0.423243	0.406256	0.391178	0.377771	0.365827	0.355163	0.345619
StageLoadir	1.358582	1.073447	0.869492	0.718589	0.603814	0.514493	0.443619	0.386441	0.339645	0.300862	0.268362	0.240857	0.217373
Flow_Coeff	0.880115	0.782325	0.704092	0.640084	0.586744	0.54161	0.502923	0.469395	0.440058	0.414172	0.391162	0.370575	0.352046
Mrel_1	0.670939	0.7205	0.772919	0.82795	0.885446	0.945335	1.007609	1.07232	1.139568	1.209502	1.28232	1.358268	1.43765

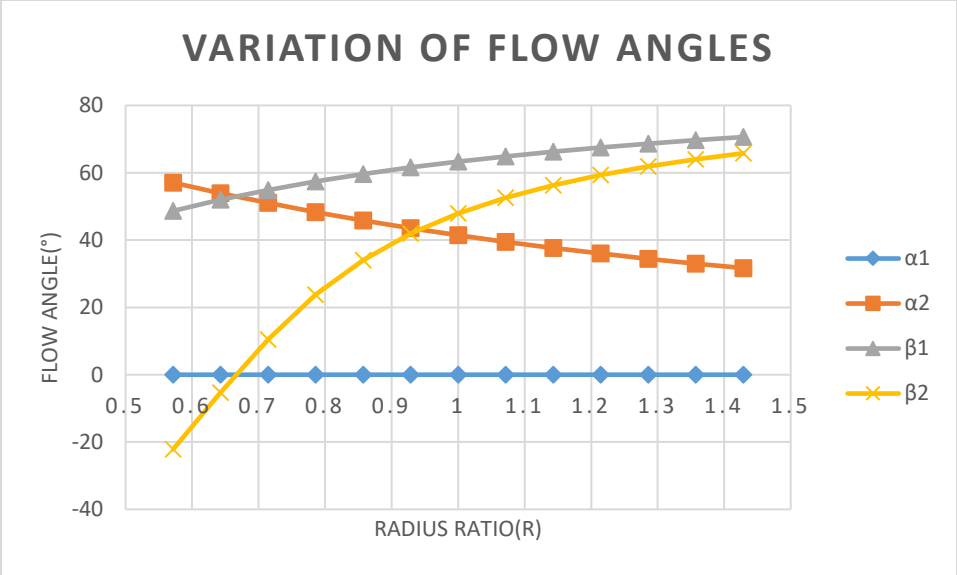

Figure 6- Variation of flow angles along annulus

- The above plot shows the increase of blade angles as we move towards the tip but the difference is small (Table-(1)), whereas at the hub, the difference is too large indicating large flow turning (β1-β2) occurring at the hub as it is used to be.

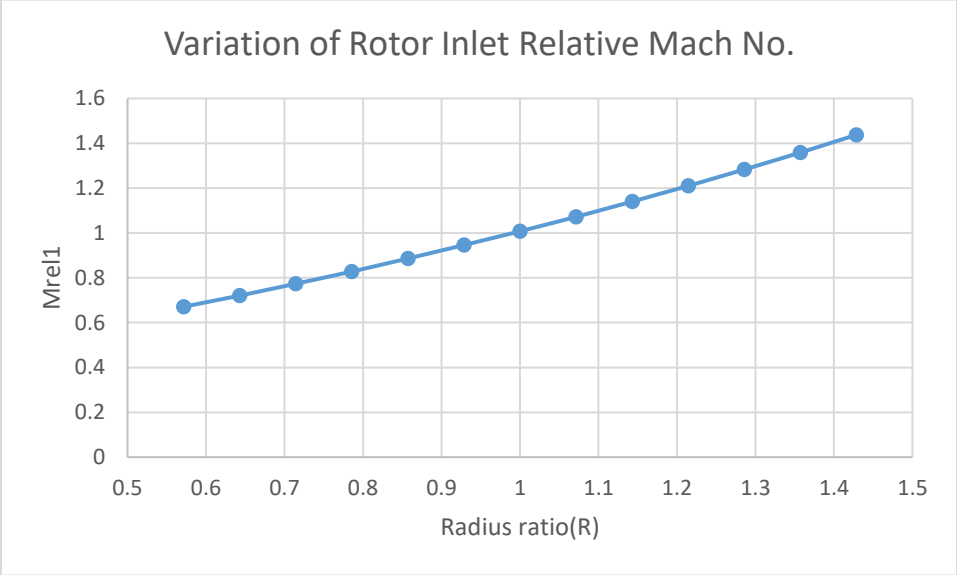

Figure 7- Variation of rotor inlet relative Mach number along annulus

- Variation of inlet rotor relative Mach number along annulus shows its increase along annulus. It is also to be noted that the M_{max} occurs at the tip with a value of 1.44 which is tend to lie within the reasonable range for transonic stage satisfying the design criteria discussed earlier. Also, it observed for a transonic stage to happen, there must be a

subsonic regime at the hub, a sonic radius in middle and supersonic regime at the tip as mentioned in the figure below.

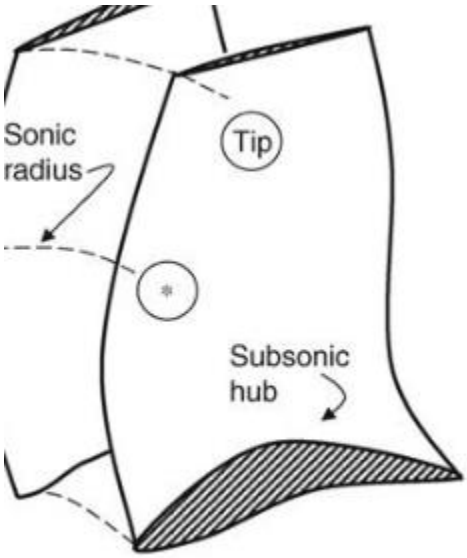

Figure 8- sketch of a transonic rotor[5]

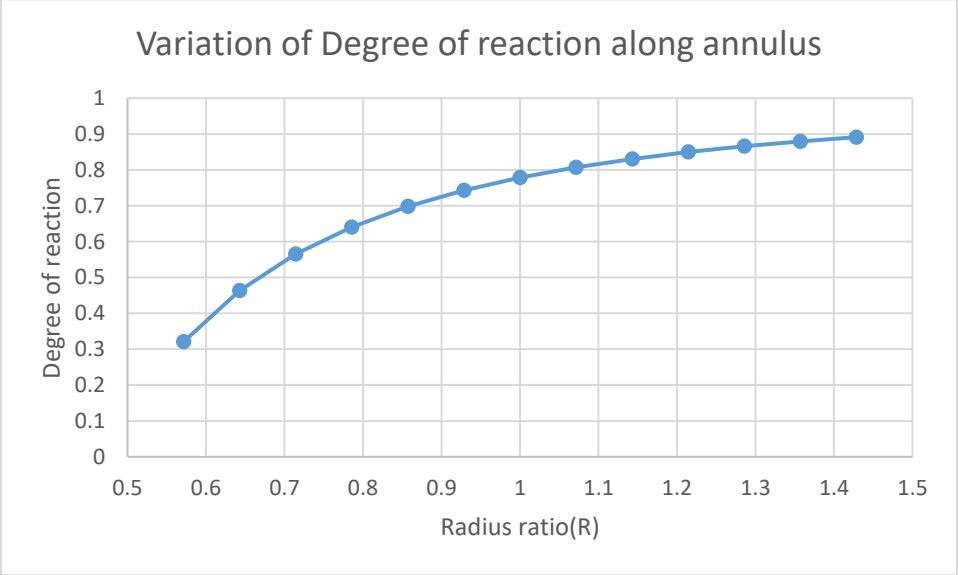

Figure 9- Variation of degree of reaction along annulus

- As per free-vortex law, the degree of reaction increases from hub to tip; This is found to be in agreement with the above plot and also large flow turning at stator hub adds to the above discussion.

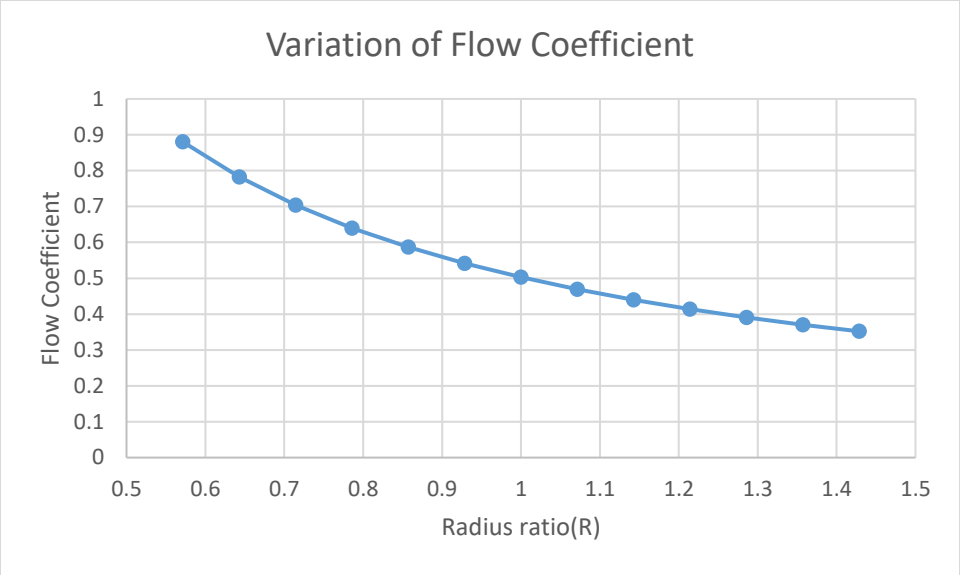

Figure 10- Variation of flow co-efficient along annulus

- By assumption of constant axial velocity and also constant axial velocity ($\frac{dca}{dr} = 0$) along annulus by free vortex law, the flow co-efficient is found to decrease along annulus due to increase in blade speed.

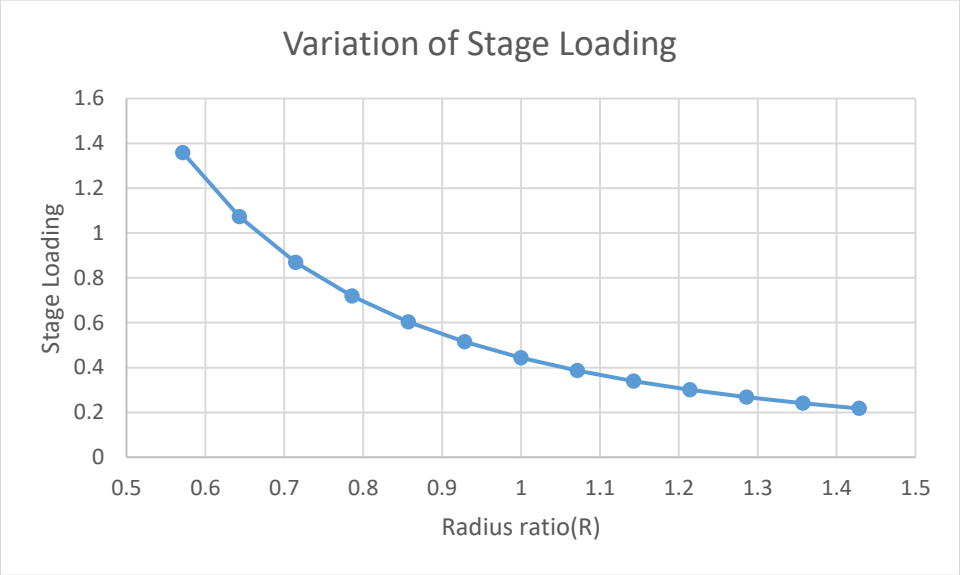

- The stage loading at the hub is found to be higher as it is used to be indicated by the plot.

- From table-1, it can be observed that the diffusion factor(D*) for both stator and rotor is within reasonable limits indicating less probability for flow separation.
- Also, both the thermodynamic work and aerodynamic works are found to be matching and is constant throughout the annulus as per free vortex law.

3.1 Blade Geometry:

The blade sections can be generated in a variety of ways in Multall.

1. A pre-existing blade shape may be input by reading in its coordinates.

2. The blade shape is input as a table of camber line angle and blade thickness against fraction of meridional chord.

The blade profiles are generated on a plane (x,y) surface but are then transformed into the (m,θ) coordinate system of the stream-wise surfaces such that the x value becomes the meridional distance m and the y value defines the value of θ on the stream-wise surface using

$$\theta - \theta_1 = \int_{r1}^{r} dy/r$$

This ensures that a flat plate on the (x,y) surface transforms into a log spiral on the (m,θ) surface.

The blade co-ordinates data generated using Multall, is included in appendix-B. Modelling tools such as CATIA and Solid-works were used for 2-D and subsequent 3-D modelling.

3.1.1 Initial blade design

The initial blade was generated with 66 stator blades. From the figure, it can be observed that the Blockage Factor will be much higher such that prescribed design mass flow rate cannot be achieved. so we changed number of blades in annular direction. The initial blade modelled

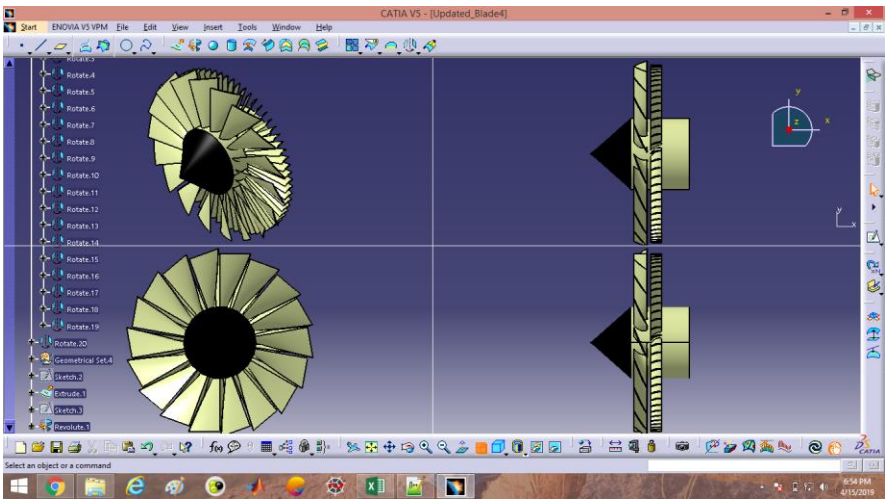

Figure 11- Isometric,Front and Side views of intial blade model

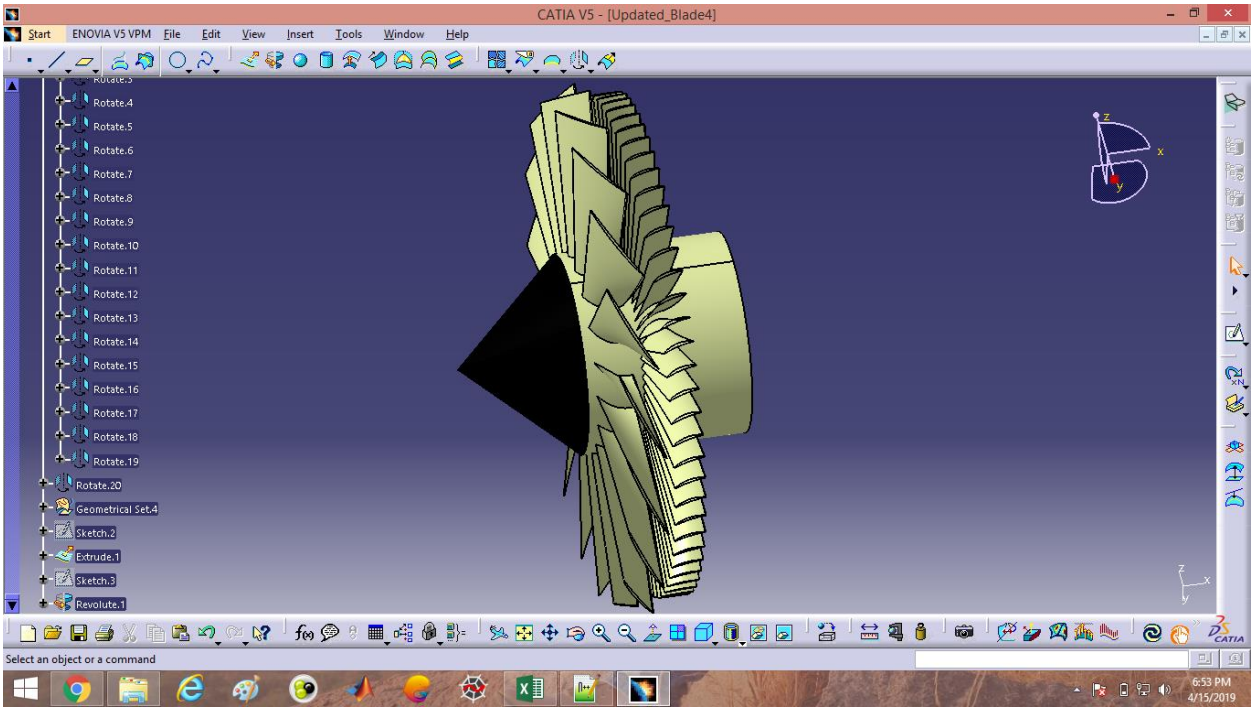

Figure 12- Isometric Side view of Initial blade model

3.1.2 Optimized(Finalized) blade design

The optimized blade generating the required mass flow was obtained by altering certain design parameters. Number of stator blades were considerably reduced (36-stator blades, 19 rotor blades) thereby accounting for the effects of increased blockage factor. Further, Aspect ratio (blade height/chord) was altered within the reasonable limits (4 to 4.5), by changing the chord length, since blade height being a fixed design parameter.

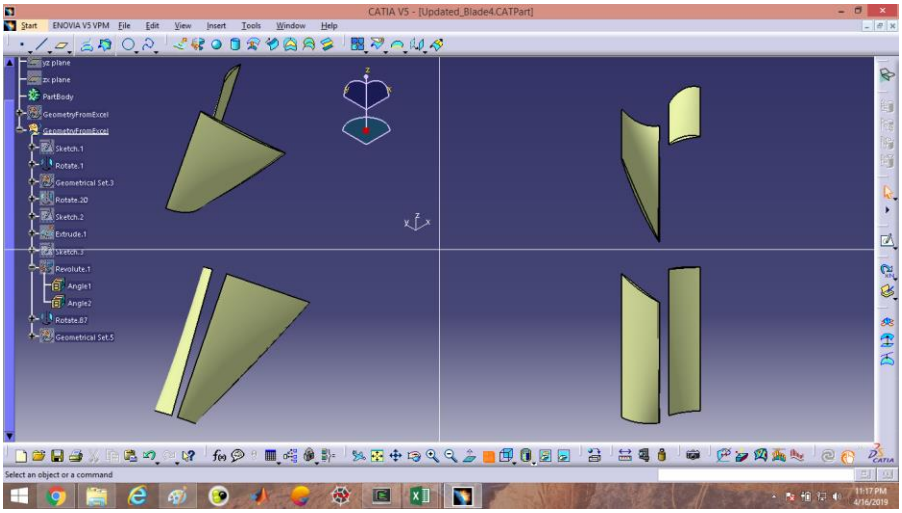

Figure 13- Rotor and stator blade (pair) arrangement

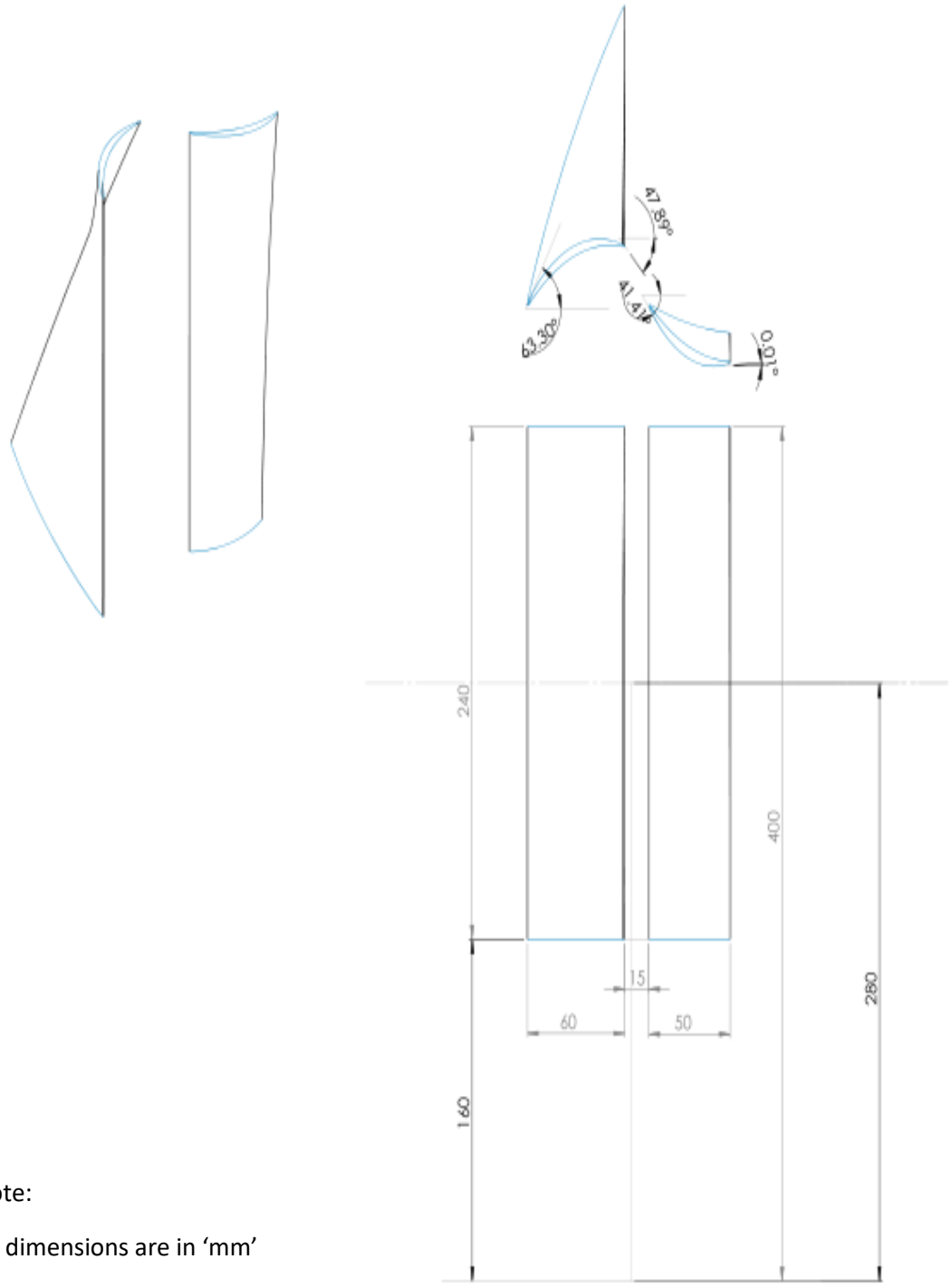

Note:

All dimensions are in ‘mm’

Figure 14- linear cascade model of a single rotor-stator pair

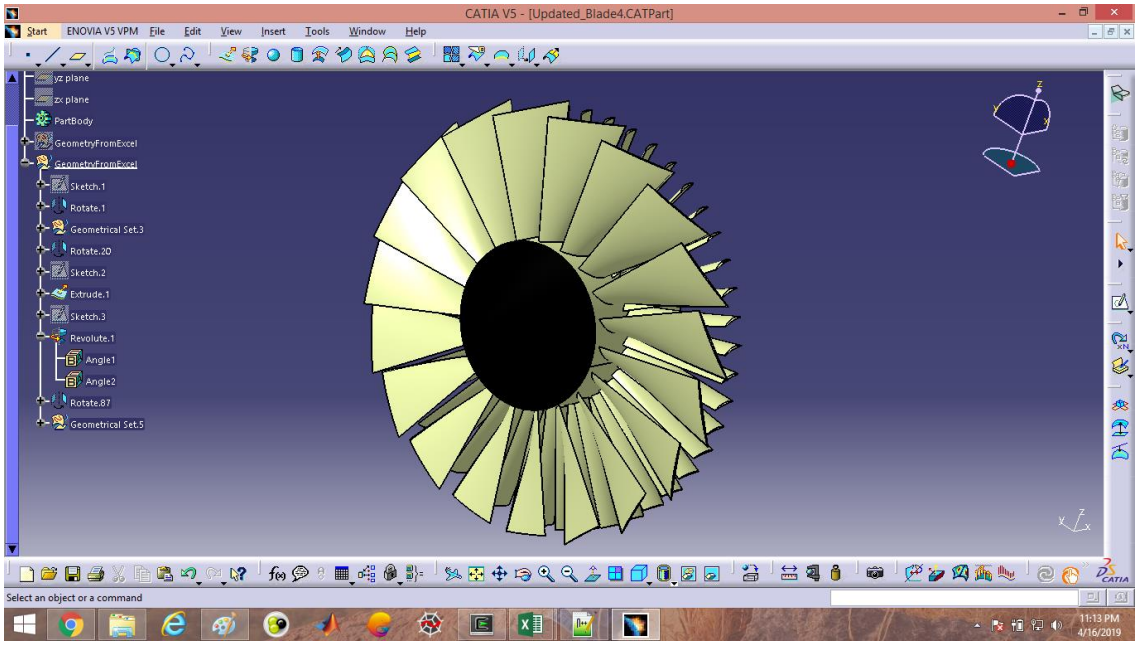

Figure 15- Front view of finalized transonic stage

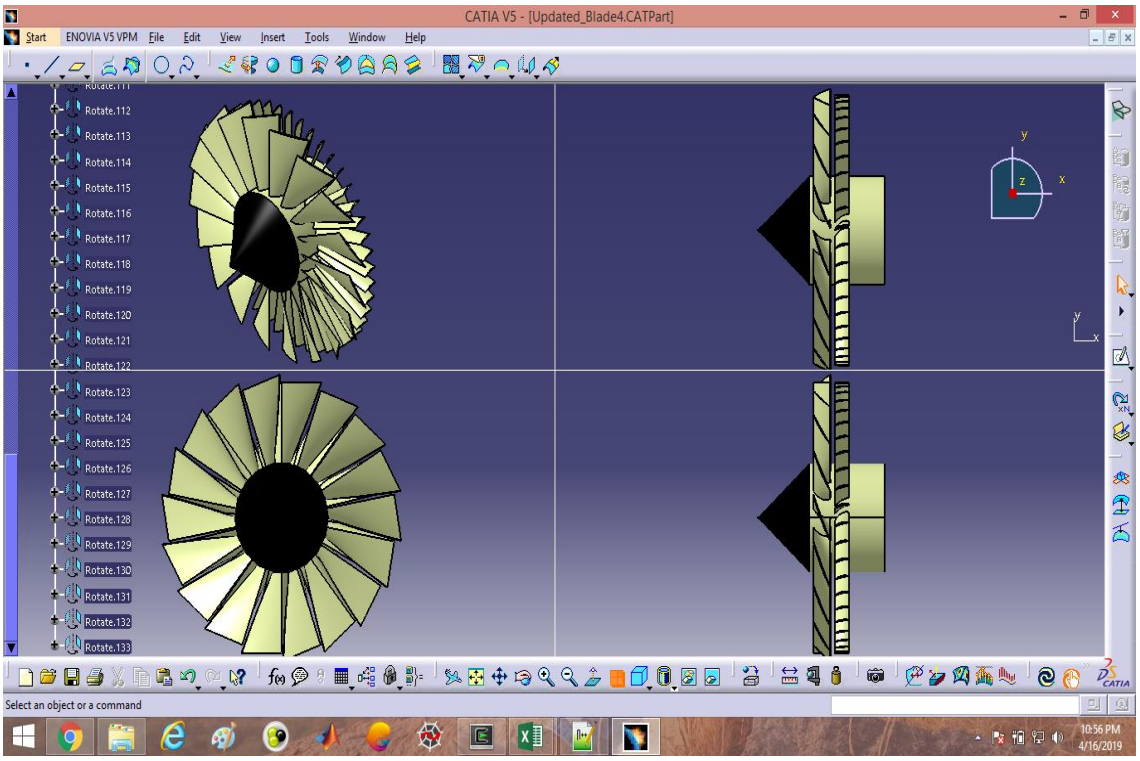

Figure 16- 3-View diagram of Finalized transonic stage

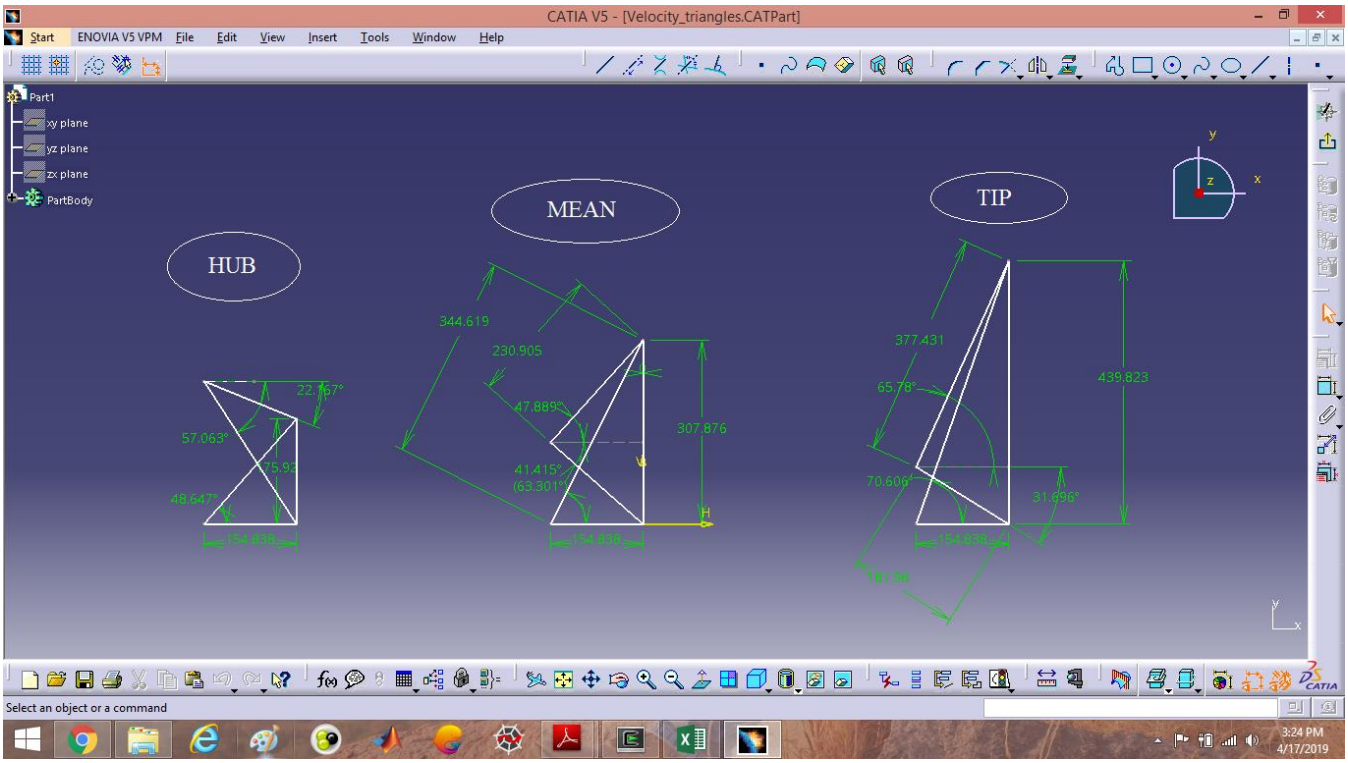

Figure 17 Velocity triangles at hub, mean and tip of finalized design

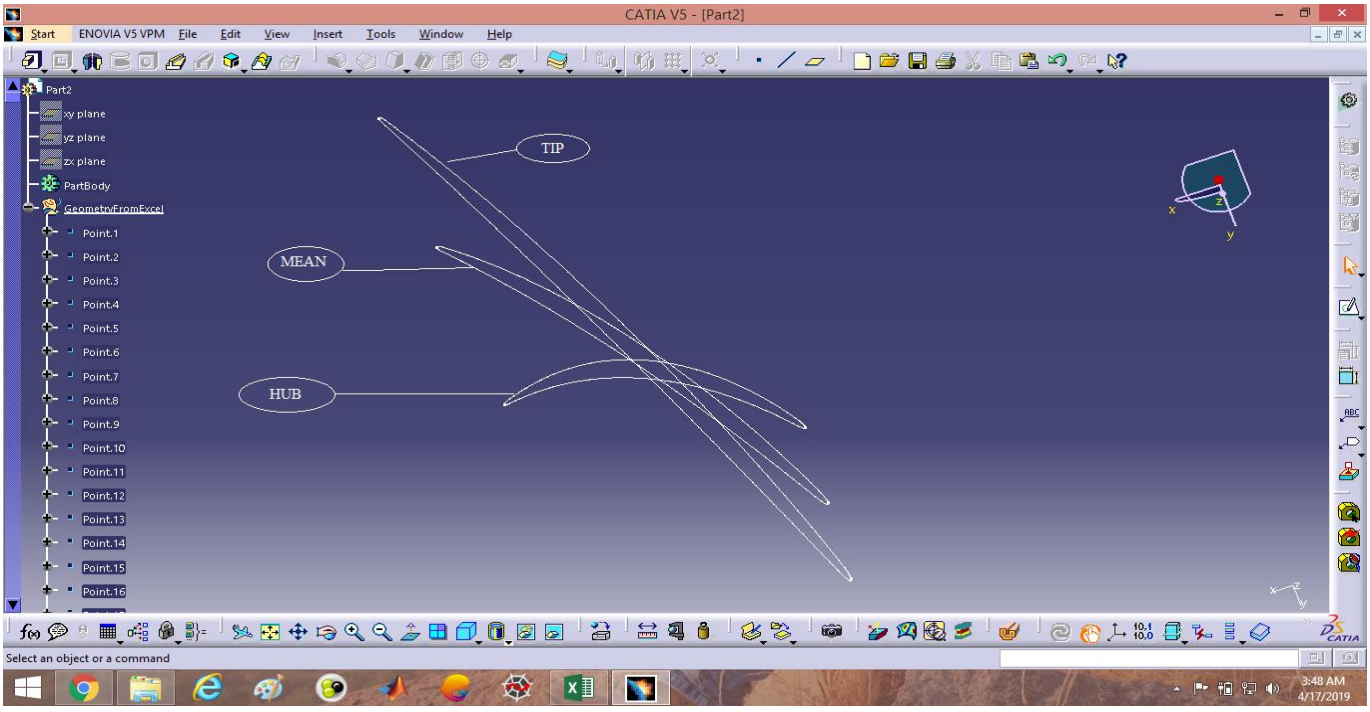

Figure 18- Blade sections at hub, mean and tip

4.Conclusion

- Manual and computational analysis have been carried out for design of transonic stage axial fan having low hub-to-tip ratio (0.4) with a rotor rotational speed of 10500 rpm.

- Certain reasonable assumptions were made during the design process and a check has been made whether such assumptions could satisfy the primitive design criteria.

- Manually, calculated 1-D design values were compared with the obtained ‘meangen’ values for given specifications and the design process is carried further.

- 3-D design analysis were carried using ‘Free Vortex Law’ and similarity comparison has been made with the ‘Stagen’ values.

- The output from ‘Stagen’ file has been given as input to ‘Multall’ file to carry out the simulation and convergence is checked (Inflow=Outflow)

- Once the convergence is met, blade geometry is finalized after appropriate optimization and 3-D CAD models were generated.

References

1. H. Cohen, HIH Saravanamuttoo, GFC Rogers, *Gas Turbine Theory*, Fifth Edition, Pearson Education Ltd.
2. Budugar Lakshminarayana, *Fluid Dynamics and Heat Transfer of Turbomachinery*, Fourth Edition.
3. NPTEL, "*Turbomachinery Aerodynamics*", by Prof.A.M.Pradeep and Prof.Baskar Roy.
4. Ahmed F. El-Sayed, *Fundamentals of Aircraft and Rocket Propulsion*, Springer Edition.
5. Class lecture slides, "*Aerodynamics of Compressors and Turbines",* by Prof.A.M.Pradeep.

Appendix-A

Test cases (1-5) data for Mean-design

Case_No	T1(K)	Ca(m/s)	P_01	T_01	ρ_01(kg/n	π_c	ηc
1	294.6594	240.8592	29988.32	323.5217	0.322974	1.5	0.9
2	294.6594	275.2676	28835.58	332.357	0.302303	1.5	0.9
3	294.6594	154.838	38644.5	306.5872	0.439189	1.5	0.86
4	294.6594	154.838	38644.5	306.5872	0.439189	1.5	0.9
5	294.6594	154.838	38644.5	306.5872	0.439189	1.5	0.9

Case_No	ρ_1(kg/m	Ca(m/s)	U_mean(r	Flow_coef	delta_h0(J	delta_T0(I	stg_loadn
1	0.255659	240.8592	307.8761	0.782325	44372.21	44.15145	0.468122
2	0.223702	275.2676	307.8761	0.894086	45584.02	45.35723	0.480907
3	0.397692	154.838	263.8938	0.586744	44005.38	43.78645	0.631899
4	0.397692	154.838	307.8761	0.502923	42049.58	41.84038	0.443619
5	0.397692	154.838	307.8761	0.502923	42049.58	41.84038	0.443619

Case_No	Alpha_2(°	DOR	Beta_1	Beta_2	Vrel_1	Mrel_1	Vrel_2
1	30.89516	0.765939	51.96304	34.21054	374.4226	1.172555	291.2525
2	28.27471	0.759547	48.20056	30.13884	397.7073	1.245743	318.2979
3	47.12204	0.684051	59.59799	32.10264	288.9543	0.885446	182.7866
4	41.41488	0.778191	63.30112	47.889	322.4406	1.00761	230.9054
5	41.41488	0.778191	63.30112	47.889	322.4406	1.00761	230.9054

Case_No	Vu_1	Vu_2	Spacing(S	Chord(m)	D*_R	C_2
1	307.8761	163.7525	0.025	0.05	0.31836	280.6862
2	307.8761	159.8165	0.025	0.05	0.292739	312.5602
3	263.8938	97.13966	0.025	0.05	0.511694	227.556
4	307.8761	171.2965	0.05	0.05	0.495673	206.4674
5	307.8761	171.2965	0.05	0.05	0.495673	206.4674

Case_No	Cu_2	C(m)	Spacing (S)(m)	
1	144.1236	0.04	0.026	
2	148.0596	0.04	0.026	
3	166.7541	0.04	0.026	
4	136.5796	0.05	0.05	
5	136.5796	0.05	0.05	

Appendix-B

Blade Geometry Co-ordinates for finalized design

The blade geometry co-ordinates for finalized design extracted from Multall is included in the following link:

BLADE GEOMETRY CO-ORDINATES